Optimization of Rectangular Tank Cross-Section Using Trust Region Gradient Method

Tomasz Garbowski[1)], Anna Szymczak-Graczyk[2*)], Janusz Rutkowski[3)]

[1)] Department of Biosystems Engineering, Poznan University of Life Sciences, Wojska Polskiego 50, 60-627 Poznań, Poland; e-mail: tomasz.garbowski@up.poznan.pl; ORCID: https://orcid.org/0000-0002-9588-2514
[2*)] Department of Construction and Geoengineering, Poznan University of Life Sciences, Piątkowska 94E, 60-649 Poznań, Poland; e-mail: anna.szymczak-graczyk@up.poznan.pl; ORCID: https://orcid.org/0000-0002-1187-9087
[3)] Department of Biosystems Engineering, Poznan University of Life Sciences, Wojska Polskiego 50, 60-627 Poznań, Poland; e-mail: janusz.rutkowski@up.poznan.pl; ORCID: https://orcid.org/0000-0003-1525-8111

http://doi.org/10.29227/IM-2024-02-26

Submission date: *31.07.2024.* | Review date: *13.07.2024*

Abstract

In various industries, rectangular tanks are commonly used for storing liquids and other materials. The design and optimization of these tanks are crucial for ensuring structural integrity and material efficiency. Traditional designs often utilize constant wall thickness, which does not align optimally with the stress distribution, leading to potential overuse of materials and increased costs. Recent studies have shown that tanks with variable wall thickness, such as trapezoidal cross-sections, can better match stress distributions, particularly under hydrostatic loads, resulting in more efficient use of materials. This research aims to build upon previous studies by introducing an advanced optimization algorithm based on the Trust Region Gradient Method to further refine the cross-sectional design of rectangular tanks. The primary objective is to minimize the material usage while maintaining structural safety and performance under various load conditions, including hydrostatic pressure and thermal effects. The proposed algorithm iteratively adjusts the tank's wall thickness, seeking an optimal configuration that reduces bending moments and material costs. Initial static calculations is verified using the finite difference method, emphasizing energy minimization conditions for elastic strain in bent plates on elastic foundations. This approach is compared with traditional discretization methods to validate accuracy. The trust region method is then applied to optimize the design, with a focus on achieving a balance between structural integrity and economic feasibility. Preliminary results indicate that the trust region gradient method can significantly enhance the design process, leading to substantial material savings and improved structural performance. The algorithm's effectiveness is demonstrated through case studies comparing tanks with constant and variable wall thickness. This research contributes to sustainable construction practices by promoting designs that use materials more efficiently and meet safety standards.

Keywords: *rectangular tanks, Trust Region Algorithm, variable wall thickness, finite difference method, structural optimization, sustainable construction*

1. Introduction

Effective water management has become a necessity in the modern world. The increasing frequency of extreme weather events such as droughts and floods is affecting larger areas, both urban and rural. In each of these places, appropriate measures must be taken to manage water resources [1,2]. Tanks are widely used structures for storing water and other products resulting from technological processes. Depending on the material used, tanks can be made of steel, concrete, or plastics. Standardization is often applied to steel and plastic tanks, less so to concrete tanks, as these tanks are ready for installation immediately upon delivery, requiring no assembly on site [3]. There has been significant development in the design of standard steel tanks for water [3], gas [4], and bulk materials [5]. This development facilitates the purchase and installation of tanks, particularly small ones, without the need for administrative permits, thus increasing the capacity for proper storage of water, grain, waste, and other products related to various activities.

Plastic and composite tanks are mainly used for storing waste and water in small facilities [6]. Standardization of reinforced concrete tanks primarily concerns smaller structures, as creating watertight joints between components in larger constructions is challenging [7]. However, in many cases, reinforced concrete tanks are designed individually, considering the guidelines and needs of the investor and user [8]. In such cases, strength considerations and the impact of stored substances on the tank walls, which can act destructively on the concrete, are crucial. Despite this, concrete remains a viable construction material for tanks, as modern technologies for protecting concrete surfaces from harmful substances stored in tanks are advancing rapidly [9,10].

Proper tank design requires knowledge of their statics and the interrelationships between components. Traditional methods, such as the method of isolated plates, divide a rectangular tank into individual plates: wall, bottom, and cover. For accuracy, if the difference in moments does not exceed 10%, the higher value is taken as representative, while greater differences require methods like Cross's method, which distributes the difference in support moments among the plates proportionally to their stiffness [7,8].

Tanks are most commonly designed with walls of constant thickness, although trapezoidal cross-section walls are optimal in terms of load-bearing capacity. This is particularly relevant in structures where the load distribution is triangular, such as with water pressure on walls. Wall thickness should increase with depth, which is economical but more challenging to construct [11]. There are numerous publications on tanks with constant wall thickness [12,13], describing proper design principles and possible errors and corrective measures [7,8].

Loads acting on tanks can be categorized as permanent, such as the self-weight and backfill soil weight for underground tanks, and variable environmental and operational loads, such as snow load, vehicle load on the ground surface, earth pressure, and soil friction on the wall for tanks constructed using the caisson method. Thermal effects, less frequently described in literature and less understood by

designers, can impact structures through uniform heating or cooling of the entire cross-section, or by creating temperature differences between the element's surfaces [14]. Thinner walls in the upper part, which are typically more exposed to thermal influences, are justified because bending moments caused by temperature differences increase proportionally to the square of the wall thickness. There is less scientific literature on tanks with linearly varying wall thickness, especially those subjected to thermal variations [15,16]. This issue has been addressed in works [11,17], which included numerical analysis of plates with tapered thickness subjected to temperature effects [17] and numerical calculations for tanks with varying wall thickness verified experimentally [11].

The aim of this work is to refine the cross-sectional design of rectangular tanks by introducing an advanced optimization algorithm based on the Trust Region Gradient Method. The primary objective is to minimize material usage while maintaining structural safety and performance under various load conditions, including hydrostatic pressure and thermal effects. The research aims to optimize the tank's wall thickness, reduce bending moments and material costs, and improve structural efficiency, thereby contributing to sustainable construction practices by promoting material-efficient designs that meet safety standards

2. Materials and Methods

2.1 Finite Difference Method – A Brief Summary

Static calculations for tanks can be performed using several popular numerical methods. These include methods such as the Boundary Element Method (BEM), the Finite Difference Method (FDM), and the Finite Element Method (FEM). Calculation software for designing structures like tanks typically relies on FEM. In this work, the FDM is used as an alternative and equally effective approach to solve the specified systems of differential equations. This method provides a highly versatile way of solving differential equations with given boundary conditions by replacing the derivatives in the equations and boundary conditions with appropriate finite differences. Since the function describing the plate deflection is unknown, the ordinates of the surface at a finite number of points, called nodes, located at the intersections of the created grid of the calculated object are taken as unknowns [18]. The topic of the Finite Difference Method was extensively covered in many outstanding and fundamental scientific works in the 1970s and 1980s [19-24], which have inspired contemporary authors [25-29]. The FDM has been used in numerical calculations for plates [17,29,30], tanks [11-13], and surface girders [31-35].

In this work, the condition for the minimum energy of elastic deformation stored in a bent plate - vertical walls of tank, resting on an elastic foundation was used. The calculations were carried out traditionally by discretizing the object and creating systems of equations. Then, using proprietary calculation solutions, results such as deflections at each point of the division grid were obtained, and bending moments at selected points were calculated.

For a thin plate of thickness h, the differential equation of the deflection surface read [18]:

$$D\nabla^2\nabla^2 w = q \tag{1}$$

where:

- $D = \frac{Eh^3}{12(1-\nu^2)}$ is the flexural rigidity of the plate,
- E is the Young's modulus,
- ν is the Poisson's ratio,
- $\nabla^2\nabla^2 w = \frac{\partial^4 w}{\partial x^4} + 2\frac{\partial^4 w}{\partial x^2 \partial y^2} + \frac{\partial^4 w}{\partial y^4}$,
- $w(x, y)$ is the transverse deflection,
- $q(x, y)$ is a transverse distributed load.

If the plate is supported by an elastic foundation with a modulus K_t (horizontal stiffness) and K_z (vertical stiffness), the plate deflection due to the foundation is:

$$w_K = -\frac{K_t h^2}{4}\nabla^2 w + K_z w \tag{2}$$

The influence of in-plane loads on the deflection of a plate.

$$w_N = -N_x\frac{\partial^2 w}{\partial x^2} - 2N_{xy}\frac{\partial^2 w}{\partial x \partial y} - N_y\frac{\partial^2 w}{\partial y^2} + p_x\frac{\partial w}{\partial x} + p_y\frac{\partial w}{\partial y} \tag{3}$$

where:

- N_x is a normal force in x direction,
- N_y is a normal force in y direction,
- N_{xy} is a shear force in x-y plane;
- p_x is a distributed load in x direction,
- p_y is a distributed load in y direction.

The deflection due to a temperature change ΔT can be accounted for by considering the thermal stresses induced in the plate.

$$q_T = -(1+\nu)\frac{D\alpha_t}{h}\nabla^2\Delta T \tag{4}$$

where α_t is the coefficient of thermal expansion. The influence of transverse forces on the deflection of a plate can be formulated:

$$q_R = -\frac{D}{H}\nabla^2\left[p_z + \frac{1}{6}\left(\frac{\partial m_x}{\partial x} + \frac{\partial m_y}{\partial y}\right)\right] \tag{5}$$

where:

- p_z is the transverse distributed load,
- m_x is a distributed moment with respect to x axis,

- m_y is a distributed moment with respect to y axis.
- $H = 5/6\, Gh$ - is a coefficient.

The coefficient D/H reads:

$$\frac{D}{H} = \frac{Eh^3}{12(1+\nu^2)}\left[\frac{5}{6}h\frac{E}{2(1+\nu)}\right]^{-1} = \frac{h^2}{5(1-\nu)} \tag{6}$$

Combining all the above expressions, we get:

$$D\nabla^2\nabla^2 w + w_N + w_K = q + q_R + q_T \tag{7}$$

If one assumes the varying stiffness or plate thickness the Equation (7) reads:

$$\nabla^2(D\nabla^2 w) - L[D(1-\nu), w] + w_N + w_K = q + q_R + q_T \tag{8}$$

where:

$$L(D(1-\nu), w) = (1-\nu)\left[\frac{\partial^2 D}{\partial x^2}\frac{\partial^2 w}{\partial y^2} - 2\frac{\partial^2 D}{\partial x \partial y}\frac{\partial^2 w}{\partial x \partial y} + \frac{\partial^2 D}{\partial y^2}\frac{\partial^2 w}{\partial x^2}\right] \tag{9}$$

In the special case where the product $D(1-\nu)$ is a linear function of the coordinates x and y, the above equation takes a simpler form:

$$\nabla^2(D\nabla^2 w) + w_N + w_K = q + q_R + q_T \tag{10}$$

Internal forces and stresses in the plate are defined as follow. The bending moments in the x and y directions, denoted as M_x and M_y, describe the internal moments generated by bending of the plate. They are given by:

$$M_x = -D\left(\frac{\partial^2 w}{\partial x^2} + \nu\frac{\partial^2 w}{\partial y^2} + (1+\nu)\frac{\alpha_t \Delta T}{h}\right) \tag{11}$$

$$M_y = -D\left(\nu\frac{\partial^2 w}{\partial x^2} + \frac{\partial^2 w}{\partial y^2} + (1+\nu)\frac{\alpha_t \Delta T}{h}\right) \tag{12}$$

The twisting moment, M_{xy}, represents the internal moment due to twisting of the plate and is given by:

$$M_{xy} = -D(1-\nu)\frac{\partial^2 w}{\partial x \partial y} \tag{13}$$

The shear forces in the x and y directions, denoted as T_x and T_y, describe the internal forces acting parallel to the plane of the plate. These are important for assessing the plate's resistance to shear stresses. They are defined as:

$$T_x = -D\left(\frac{\partial^3 w}{\partial x^3} + (2+\nu)\frac{\partial^3 w}{\partial x \partial y^2}\right) - (1-\nu)\frac{D\alpha_t}{h}\frac{\partial \Delta T}{\partial x} \tag{14}$$

$$T_y = -D\left(\frac{\partial^3 w}{\partial y^3} + (2+\nu)\frac{\partial^3 w}{\partial y \partial x^2}\right) - (1-\nu)\frac{D\alpha_t}{h}\frac{\partial \Delta T}{\partial y} \tag{15}$$

Normal stresses in the plate in the x and y directions, denoted as σ_x and σ_y, are derived from the bending moments and describe the internal stress distribution across the thickness of the plate. They are defined as:

$$\sigma_x = -\frac{E}{1-\nu^2}\left[z\left(\frac{\partial^2 w}{\partial x^2} + \nu\frac{\partial^2 w}{\partial y^2}\right)\right] = \frac{6}{h^2}M_x \tag{16}$$

$$\sigma_y = \frac{E}{1-\nu^2}\left[z\left(\nu\frac{\partial^2 w}{\partial x^2} + \frac{\partial^2 w}{\partial y^2}\right)\right] = \frac{6}{h^2}M_y \tag{17}$$

The solution to the plate bending problem involves finding the deflection $w(x, y)$ that minimizes this functional, subject to the appropriate boundary conditions. For example, Equation (1) can be written using the central finite difference method as follows:

$$D\left(\frac{\Delta^4 w_i}{\Delta x^4} + 2\frac{\Delta^4 w_{ij}}{\Delta x^2 \Delta y^2} + \frac{\Delta^4 w_j}{\Delta y^4}\right) = q_{i,j} \tag{18}$$

where:

$$\Delta^4 w_i = w_{i-2,j} - 4w_{i-1,j} + 6w_{i,j} - 4w_{i+1,j} + w_{i+2,j} \tag{19}$$

$$\Delta^4 w_{ij} = w_{i-1,j-1} + w_{i-1,j+1} + w_{i+1,j-1} + w_{i+1,j+1} - 2\left(w_{i-1,j} + w_{i,j-1} + w_{i+1,j} + w_{i,j+1}\right) + 4_{w_{i,j}} \tag{20}$$

$$\Delta^4 w_j = w_{i,j-2} - 4w_{i,j-1} + 6w_{i,j} - 4w_{i,j+1} + w_{i,j+2} \tag{21}$$

Assuming that the stiffness or the plate thickness may vary along the x or y direction, Equation (1) takes the form:

$$\nabla^2(D\nabla^2 w)_{i,j} = q_{i,j} \tag{22}$$

In this equation, the term D, representing the flexural rigidity of the plate, is a function of the spatial coordinates x and y. This variation is incorporated into the finite difference approximation, resulting in a more complex but accurate representation of the plate's behavior. The expanded finite difference form of the equation is:

$$\nabla^2(D\nabla^2 w)_{i,j} \approx \frac{L_{i+1,j}-2L_{i,j}+L_{i-1,j}}{\Delta x^2} + \frac{L_{i,j+1}-2L_{i,j}+L_{i,j-1}}{\Delta y^2} \tag{23}$$

where:

$$L_{i,j} = D_{i,j}\left(\frac{w_{i+1,j}-2w_{i,j}+w_{i-1,j}}{\Delta x^2} + \frac{w_{i,j+1}-2w_{i,j}+w_{i,j-1}}{\Delta y^2}\right) \tag{24}$$

$$L_{i-1,j} = D_{i-1,j}\left(\frac{w_{i,j}-2w_{i-1,j}+w_{i-2,j}}{\Delta x^2} + \frac{w_{i-1,j+1}-2w_{i-1,j}+w_{i-1,j-1}}{\Delta y^2}\right) \tag{25}$$

$$L_{i+1,j} = D_{i+1,j}\left(\frac{w_{i+2,j}-2w_{i+1,j}+w_{i,j}}{\Delta x^2} + \frac{w_{i+1,j+1}-2w_{i+1,j}+w_{i+1,j-1}}{\Delta y^2}\right) \tag{26}$$

$$L_{i,j+1} = D_{i,j+1}\left(\frac{w_{i+1,j+1}-2w_{i,j+1}+w_{i-1,j+1}}{\Delta x^2} + \frac{w_{i,j+2}-2w_{i,j+1}+w_{i,j}}{\Delta y^2}\right) \tag{27}$$

$$L_{i,j-1} = D_{i,j-1}\left(\frac{w_{i+1,j-1}-2w_{i,j-1}+w_{i-1,j-1}}{\Delta x^2} + \frac{w_{i,j}-2w_{i,j-1}+w_{i,j-2}}{\Delta y^2}\right) \tag{28}$$

Since the tank walls are analyzed individually, treated as plates fixed at the two side edges and the bottom edge, while the top edge remains free. Establishing appropriate boundary conditions in the differential equations is crucial for accurate analysis. These boundary conditions ensure the physical constraints and behaviors of the tank walls are properly represented in the mathematical model, leading to precise and reliable results in the static calculations. This approach allows for a detailed understanding of the stress distribution and deformation of the tank walls under various loading conditions.

In the finite difference method analysis of the tank walls, it is essential to define specific boundary conditions for both types of edges: fixed and free. At the fixed edges, the displacements in all directions (horizontal and vertical) are set to zero. This means that the nodes along these edges cannot move or rotate, see Equation (29):

$$w_{i,j} = 0 \tag{29}$$

The rotational displacement or slope at these edges is also set to zero, ensuring that there is no angular change at the points of fixation. Equation (30)-(31) shows no rotation with respect the x-axis and y-axis, respectivelly:

$$(\phi_x)_{i,j} = \frac{-w_{i-1,j}+w_{i+1,j}}{2\Delta x} = 0 \tag{30}$$

$$(\phi_y)_{i,j} = \frac{-w_{i,j-1}+w_{i,j+1}}{2\Delta y} = 0 \tag{31}$$

These conditions simulate the physical scenario where the tank walls are rigidly attached to the surrounding structure, preventing any form of movement or deformation at the fixed edges.

Along the free edge p, the shear force and bending moment are zero. This reflects the absence of external constraints or supports, allowing the edge to move freely. There is no restriction on the displacement along the free edge, meaning it can deform under the applied loads. These conditions replicate the real-world situation where the top edge of the tank wall is not restrained, allowing it to respond freely to the internal water pressure and other forces.

$$(M)_p = 0 \tag{32}$$

$$(T)_p = 0 \tag{33}$$

Having calculates deflections in all internal nodes of the plate, internal forces and stresses can be computed using again central finite difference scheme:

$$(M_x)_{i,j} = D_{i,j}\left(\frac{w_{i-1,j}-2w_{i,j}+w_{i+1,j}}{\Delta x^2} + \nu\frac{w_{i,j-1}-2w_{i,j}+w_{i,j+1}}{\Delta y^2}\right) \tag{34}$$

$$\left(M_y\right)_{i,j} = D_{i,j}\left(\nu\frac{w_{i-1,j}-2w_{i,j}+w_{i+1,j}}{\Delta x^2} + \frac{w_{i,j-1}-2w_{i,j}+w_{i,j+1}}{\Delta y^2}\right) \tag{35}$$

$$(T_x)_{i,j} = -D\left[\frac{\Delta^3 w_i}{2\Delta x^3} + (2-\nu)\left(-\frac{w_{i-1,j-1}-2w_{i-1,j}+w_{i-1,j+1}}{\Delta y^2} + \frac{w_{i+1,j-1}-2w_{i+1,j}+w_{i+1,j+1}}{\Delta y^2}\right)\frac{1}{2\Delta x}\right] = 0 \tag{36}$$

$$\left(T_y\right)_{i,j} = -D\left[\frac{\Delta^3 w_j}{2\Delta y^3} + (2-\nu)\left(-\frac{w_{i-1,j-1}-2w_{i,j-1}+w_{i+1,j-1}}{\Delta x^2} + \frac{w_{i-1,j+1}-2w_{i,j+1}+w_{i+1,j+1}}{\Delta x^2}\right)\frac{1}{2\Delta y}\right] = 0 \tag{37}$$

$$(\sigma_x)_{i,j} = \frac{6}{h_{i,j}^2}(M_x)_{i,j} \tag{38}$$

$$\left(\sigma_y\right)_{i,j} = \frac{6}{h_{i,j}^2}\left(M_y\right)_{i,j} \tag{39}$$

where:

$$\Delta^3 w_i = -w_{i-2,j} + 2w_{i-1,j} - 2w_{i+1,j} + w_{i+2,j} \tag{40}$$

$$\Delta^3 w_j = -w_{i,j-2} + 2w_{i,j-1} - 2w_{i,j+1} + w_{i,j+2} \tag{41}$$

2.2 Trust Region Method for Optimization of Plate Thickness in Tanks

The Trust Region Method is an iterative optimization technique used to find the minimum (or maximum) of a function. This method is particularly suitable for optimizing the linearly varying thickness of plates in tanks, where the objective is to minimize stress or deflection while maintaining structural integrity. In the trust region method, at each iteration, a quadratic model is typically used to approximate the objective function within a neighborhood of the current iterate. The size of this neighborhood is called the "trust region". The method then determines the step to take by solving a subproblem that minimizes the model within the trust region.

Given an objective function $f(t)$ that represents the stress or deflection in the tank plate, and its quadratic approximation $m_k(p)$ at the current thickness distribution t_k, the trust region subproblem is defined as:

$$\min_p m_k(p) = \nabla f(t_k)^T p + \frac{1}{2}\, p^T\, B_k\, p \tag{42}$$

subject to:

$$\|p\| \leq \Delta_k \tag{43}$$

where:

- $\nabla f(t_k)$ is the gradient of f with respect to the thickness distribution t at t_k,
- B_k is an approximation of the Hessian matrix (second derivatives) at t_k,
- p is the step to be determined,
- Δ_k is the trust region radius.

For plates with linearly varying thickness, the thickness $t(x)$ can be expressed as a linear function:

$$t(x) = t_{top} + \left(\frac{t_{bot} - t_{top}}{H}\right) x \tag{44}$$

where t_{top} and t_{bot} are the thicknesses at the top and bottom edges of the plate, respectively, and H is the height of the plate.

The objective function $f(t)$ in this context might represent the total potential energy, the maximum deflection, or the maximum stress in the plate. The goal is to find the optimal t_{top} and t_{bot} that minimize this objective function while satisfying structural constraints. After solving the subproblem and obtaining the step p_k, the new thicknss distribution is calculated as $t_{k+1} = t_k + p_k$. The actual reduction in the objective function is compared with the predicted reduction:

$$\rho_k = \frac{f(t_k) - f(t_k + p_k)}{m_k(0) - m_k(p_k)} \tag{45}$$

Depending on the value of ρ_k, the trust region radius Δ_k is updated:

- If ρ_k is close to 1, the model is good, and the trust region may be expanded.
- If ρ_k is close to 0, the model is poor, and the trust region is shrunk.

The Trust Region Method is a robust optimization technique particularly effective for problems where the objective function is difficult to approximate accurately over large regions. By iteratively adjusting the trust region size, the method ensures reliable convergence to an optimal thickness distribution, resulting in minimized stress or deflection for plates with linearly varying thickness in tanks.

3. Results

In this study, we performed a series of numerical analyses to determine the optimal thickness distribution for tank walls of various heights and widths. Specifically, we analyzed tank walls with heights H=3, 4, and 5 meters. For each height, the width of the wall was varied in proportion to the height, from $L = 1 \times H$ to $L = 3 \times H$, in increments of one meter. For each geometric configuration of the wall, the Trust Region algorithm was employed to find the optimal thicknesses at the top (h_{top}) and bottom (h_{bot}) of the wall. The objective was to minimize stress and deflection while maintaining structural integrity under a uniform liquid pressure. The liquid has a assumed density of 1000 kg/m^3, resulting in a hydrostatic pressure distribution along the height of the wall.

FDM calculations were performed for Poisson's ratio $\nu = 0$. The analysis considered a tank with a linearly varying wall thickness, being h_{top} at the top and h_{bot} at the bottom (Figure 1).

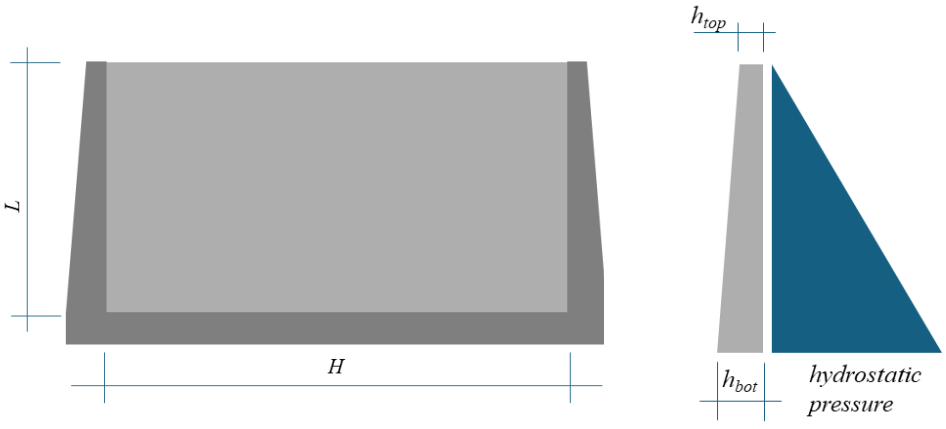

(a) (b)

Fig. 1 The tank's wall geometry and loading.

For the assumed grid of the selected wall of the tank, which has fixed divisions (dx=dy=0.25m) along the height (y direction) and width (x direction) of the plate, the wall thicknesses in each grid cell were calculated using general formulas (see Equation (22)-(33)). After solving the system of linear equations (see [18] for more details), the deflection values at all nodes of the grid for the tank with linearly varying wall thickness were obtained. Based on the deflections, bending moments and stresses were calculated using Formulas (34)-(41).

To ensure a comprehensive comparison, we also determined the constant wall thickness that would produce similar performance metrics. The constant thickness was calculated to match the criteria used in the previous analyses with linearly varying thickness. This allowed us to directly compare the effectiveness of the optimized linearly varying thickness against a uniform thickness throughout the wall's height. Table 1 presents the results of the analyses, showing the optimal thicknesses and corresponding stress and material usage values for each configuration.

Tab. 1. Optimal value of wall's thickness for various wall geometries.

H [m]	L [m]	h_{top} [m]	h_{bot} [m]	max σ_t [MPa]	material m^3/m	h_{const} [m]	max σ_t [MPa]	material m^3/m	savings [%]
3	3	0.10	0.15	2.877	0.375	0.13	2.710	0.390	3.8
3	4	0.12	0.20	2.947	0.480	0.17	2.768	0.510	5.9
3	5	0.17	0.20	2.934	0.555	0.20	2.801	0.600	7.5
3	6	0.20	0.25	2.795	0.675	0.23	2.868	0.690	2.2
3	7	0.22	0.30	2.877	0.780	0.26	2.880	0.780	0.0
3	8	0.25	0.30	2.903	0.825	0.28	2.980	0.840	1.8
3	9	0.27	0.30	2.934	0.855	0.30	2.929	0.900	5.0
4	4	0.19	0.20	2.861	0.780	0.20	2.908	0.800	2.5
4	5	0.19	0.30	2.602	0.980	0.25	2.805	1.000	2.0
4	6	0.23	0.30	2.949	1.060	0.28	2.903	1.120	5.4
4	7	0.29	0.30	2.866	1.180	0.32	2.831	1.280	7.8
4	8	0.30	0.40	2.854	1.400	0.35	2.958	1.400	0.0
4	9	0.34	0.40	2.965	1.480	0.39	2.888	1.560	5.1
4	10	0.38	0.40	2.960	1.560	0.42	2.909	1.680	7.1
4	11	0.40	0.45	2.900	1.700	0.44	2.981	1.760	3.4
4	12	0.41	0.50	2.888	1.820	0.46	2.969	1.840	1.1
5	5	0.24	0.30	2.926	1.350	0.29	2.806	1.450	6.9
5	6	0.30	0.35	2.609	1.625	0.33	2.990	1.650	1.5
5	7	0.30	0.40	2.975	1.750	0.37	2.948	1.850	5.4
5	8	0.37	0.40	2.888	1.925	0.41	2.930	2.050	6.1
5	9	0.40	0.45	2.930	2.125	0.45	2.940	2.250	5.6
5	10	0.43	0.50	2.994	2.325	0.49	2.957	2.450	5.1
5	11	0.49	0.50	2.920	2.475	0.53	2.957	2.650	6.6
5	12	0.50	0.60	2.938	2.750	0.57	2.921	2.850	3.5
5	13	0.54	0.60	2.937	2.850	0.58	2.939	2.900	1.7
5	14	0.57	0.60	2.959	2.925	0.59	2.998	2.950	0.8
5	15	0.60	0.60	2.917	3.000	0.60	2,917	3.000	0.0

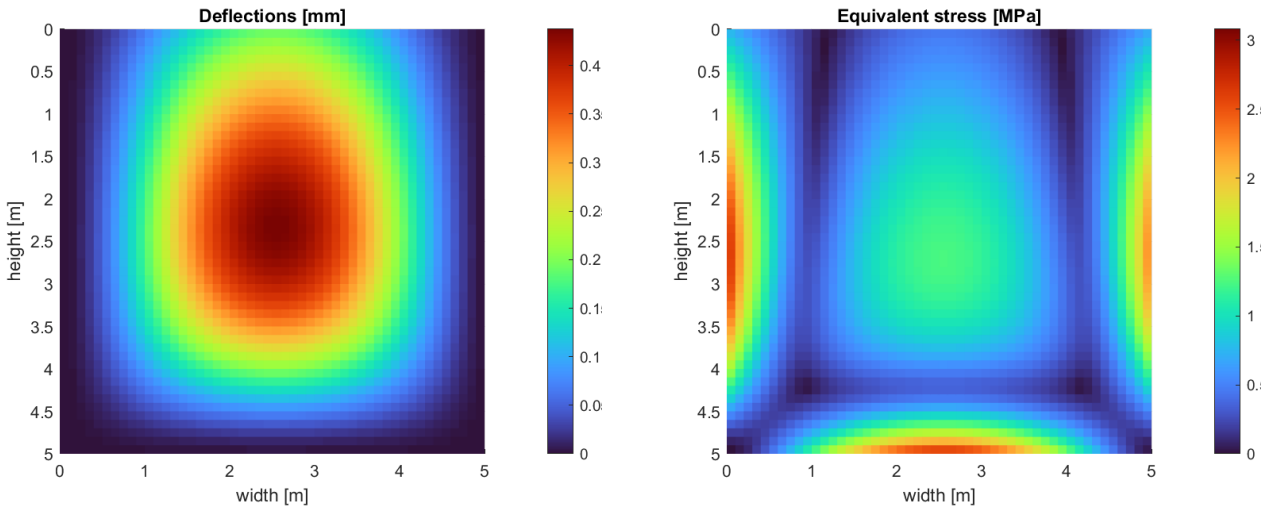

(a) (b)

Fig. 2. Displacements and stresses in selected tank's wall (5×5 m) with refined mesh dx=dy=0.1m.

4. Discussion

The numerical analyses revealed several key insights. The Trust Region algorithm effectively identified optimal thickness distributions for each wall configuration. Thicker sections were generally found at the bottom of the walls, where the hydrostatic pressure is greatest, while thinner sections were sufficient at the top. Walls with linearly varying thickness showed better performance in terms of reduced maximum stress and deflection compared to walls with uniform thickness. The optimized

configurations often required less material, providing a more efficient design without compromising structural integrity. As the height of the wall increased, the benefits of using an optimized thickness distribution became more pronounced. Wider walls required a more nuanced optimization approach to balance the increased load distribution. Figure 2 illustrates several selected stress and displacement maps for the tank walls, highlighting the differences between the optimized and constant thickness designs.

The results from Table 1 and the stress and displacement maps in Figure 2 indicate that the optimization led to material savings, particularly for taller and wider walls, where the difference between the optimized and constant thickness designs was most significant. This efficiency can translate into cost savings and more sustainable construction practices. The analysis also showed that the ratio of height to width of the wall significantly impacts the distribution of moments and stresses. Specifically, wider walls behaved more like cantilevers, with significantly higher vertical stresses. This suggests that for constructing a tank with a selected volume, ensuring appropriate ratios of wall width to tank height is crucial. This consideration is essential to prevent excessive stresses and ensure the structural integrity of the tank.

It is evident that as the width of the wall increases relative to its height, the structural behavior shifts, resulting in higher vertical stresses. Therefore, when designing tanks of a specific volume, careful attention must be given to the width-to-height ratios of the walls. Adequate proportions can help in mitigating stress concentrations and achieving a more balanced distribution of forces. This aspect of design is critical for maintaining safety and durability, particularly in large-scale tank structures.

5. Conclusions

This study demonstrates the effectiveness of the Trust Region algorithm in optimizing the thickness of tank walls with linearly varying thickness. By applying this method, significant improvements in structural performance and material efficiency were achieved. The comparison between optimized varying thickness and constant thickness designs validated the advantages of the optimization process. The results underscore the importance of considering the height-to-width ratio of the walls to manage stress distribution effectively. These findings highlight the potential for cost savings and enhanced safety in tank design, emphasizing the need for precise optimization techniques in structural engineering practices. The study provides a robust framework for future research and practical applications in the optimization of tank wall thicknesses.

References

1. I. Laks, Z. Walczak and N. Walczak, “Fuzzy analytical hierarchy process methods in changing the damming level of a small hydropower plant: Case study of Rosko SHP in Poland”, Water Resour. Ind., 29, 100204 (2023). doi: 10.1016/j.wri.2023.100204.
2. I. Laks and Z. Walczak, “Efficiency of Polder Modernization for Flood Protection. Case Study of Golina Polder (Poland)”, Sustainability, 12, 8056 (2020). doi: 10.3390/su12198056.
3. J. Ziólko, J. “Zbiorniki, silosy”, in Poradnik projektanta konstrukcji metalowych: Tom II, edited by W. Bogucki (Arkady, Warszawa, 1983).
4. J. Ziółko, Zbiorniki metalowe na ciecze i gazy (Arkady, Warszawa, 1986).
5. P. Horajski, L. Bohdal, L. Kukielka, R. Patyk, P. Kaldunski, and S. Legutko, “Advanced Structural and Technological Method of Reducing Distortion in Thin-Walled Welded Structures”, Materials 14, 504 (2021). doi: 10.3390/ma14030504.
6. W. Buczkowski, H. Mikołajczak and A. Szymczak-Graczyk, “Przykładowa ocena rozwiązań materiałowo-konstrukcyjnych zbiorników cylindrycznych z żywic poliestrowo-szklanych stosowanych w przydomowych oczyszczalniach ścieków”, Gaz, Woda i Technika Sanitarna, 12, 25-28 (2005).
7. A. Halicka and D. Franczak, Projektowanie zbiorników żelbetowych. Tom 1. Zbior¬niki na materiały sypkie (Wydawnictwo Naukowe PWN. Warszawa 2011).
8. A. Halicka and D. Franczak, Projektowanie zbiorników żelbetowych. Tom 2. Zbior¬niki na ciecze (Wydawnictwo Naukowe PWN, Warszawa 2014).
9. M. Sybis and E. Konował, “Influence of Modified Starch Admixtures on Selected Physicochemical Properties of Cement Composites”, Materials, 21, 7604 (2022). doi: 10.3390/ma15217604.
10. M. Sybis, E. Konował and K. Prochaska, “Dextrins as green and biodegradable modifiers of physicochemical properties of cement composites”, Energies, 11, 4115 (2022). doi: 10.3390/en15114115.
11. W. Buczkowski, A. Szymczak-Graczyk and Z. Walczak, “Experimental validation of numerical static calculations for a monolithic rectangular tank with walls of trapezoidal cross-section”, Bull. Pol. Acad. Sci. Tech. Sci. 65, 799–804 (2017). doi:10.1515/bpasts-2017-0088.
12. A. Szymczak-Graczyk, “Numerical Analysis of the Bottom Thickness of Closed Rectangular Tanks Used as Pontoons”. Appl. Sci., 10 (22), 8082 (2020). doi:10.3390/app10228082.
13. A. Szymczak-Graczyk, “Floating platforms made of monolithic closed rectangular tanks”. Bull. Pol. Acad. Sci. Tech. Sci., 66, 209–219 (2018). doi:10.24425/122101.
14. W. Buczkowski and A. Szymczak-Graczyk, “Monolityczne zbiorniki prostopadłościenne obciążone temperaturą”, Przegląd Budowlany, 9, 24-29 (2020).
15. W. Buczkowski, “On reinforcement of temperature loaded rectangular slabs”. Arch. Civ. Eng., 54 (2), 315-331 (2008).

16. W. Buczkowski, S. Czajka and T. Pawlak, “Analiza pracy statycznej zbiornika prostopadłościennego poddanego działaniu temperatury”, Acta Sci. Pol., Archit., 5 (2), 17-29 (2006).
17. A. Szymczak-Graczyk, “Rectangular plates of a trapezoidal cross-section subjected to thermal load”, IOP Conf. Ser. Mater. Sci. Eng., 603, 032095 (2019). doi:10.1088/1757-899X/603/3/032095.
18. Z. Kączkowski, Plates. Static Calculations (Arkady, Warszawa, Poland, 2000).
19. L. H. Donnell, Beams, Plates and Shells (McGraw-Hill, New York, NY, USA, 1976).
20. P. M. Naghdi, The Theory of Shells and Plates (Handbuch der Physick, Berlin, Germany, 1972).
21. V. Panc, Theries of Elastic Plates (Academia: Prague, Czech Republic, 1975).
22. S. Timoshenko, S. Woinowsky-Krieger, Theory of Plates and Coatings (Arkady, Warszawa, Poland, 1962).
23. R. Szlilard, Theory and Analysis of Plates. Classical and Numerical Methods (Prentice Hall, Englewood Cliffs: Bergen, NJ, USA; Prentice-Hall: Upper Saddle River, NJ, USA, 1974).
24. A. C. Ugural, Stresses in Plates and Shells (McGraw-Hill: New York, NY, USA, 1981).
25. M. Son, H. Sang Jung, H. Hee Yoon, D. Sung and J. Suck Kim, “Numerical Study on Scale Effect of Repetitive Plate-Loading”, Test. Appl. Sci., 9, 4442 (2019). doi:10.3390/app9204442-19.
26. B. E. Rapp, “Finite Difference Method”, in Microfluidics: Modelling, Mechanics and Mathematics, Micro and Nano Technologies, edited by B. E. Rapp (Elsevier, Amsterdam, The Netherlands, 2017), pp. 623–631. doi:10.1016/B978-1-4557-3141-1.50030-7.
27. J. Blazek, “Principles of Solution of the Governing Equations”, in Computational Fluid Dynamics: Principles and Applications, edited by J. Blazek (Elsevier, Amsterdam, The Netherlands, 2015), pp. 29–72. doi:10.1016/B978-0-08-099995-1.00003-8.
28. M. H. Sadd, “Formulation and Solution Strategies”, in Elasticity, Theory, Applications, and Numerics, edited by M. H. Sadd (Academic Press, Elsevier, Cambridge, Massachusetts, USA, 2005), pp. 83–102. doi:10.1016/B978-012605811-6/50006-3.
29. K. S. Numayr, R. H. Haddad and M. A. Haddad, “Free vibration of composite plates using the finite difference method”, Thin-Walled Struct., 42, 399–414 (2004). doi:10.1016/j.tws.2003.07.001.
30. A. Szymczak-Graczyk, “Numerical analysis of the impact of thermal spray insulation solutions on floor loading”, Appl. Sci., 10(3), 1016 (2020). doi: 10.3390/app10031016.
31. W. Buczkowski and A. Szymczak-Graczyk “Wpływ różnej grubości i konstrukcji ścian na pracę statyczną monolitycznych zbiorników prostopadłościennych”, Acta Sci. Pol., Archit., 7(3) (2008), pp. 23-34.
32. N. Staszak, T. Garbowski and A. Szymczak-Graczyk, “Solid Truss to Shell Numerical Homogenization of Prefabricated Composite Slabs”, Materials 14, 4120 (2021). doi: 10.3390/ma14154120.
33. N. Staszak, A. Szymczak-Graczyk and T. Garbowski, “Elastic Analysis of Three-Layer Concrete Slab Based on Numerical Homogenization with an Analytical Shear Correction Factor”, Appl. Sci., 12, 9918 (2022). doi: 10.3390/app12199918.
34. N. Staszak, T. Garbowski and B. Ksit, “Optimal Design of Bubble Deck Concrete Slabs: Sensitivity Analysis and Numerical Homogenization”, Materials, 16, 2320 (2023). doi: 10.3390/ma16062320.
35. N. Staszak, T. Garbowski and B. Ksit, “Application of the generalized nonlinear constitutive law in numerical analysis of hollow-core slabs”, Arch. Civ. Eng., 68 (2) (2022), pp. 125-145. doi: 10.24425/ace.2022.140633.